Direct probing magnetization reversal of exchange-coupled-composite media by x-ray magnetic circular dichroism

Hao-Cheng Hou, Dieter Suess, Jung-Wei Liao, Meng-Shian Lin, Hong-Ji Lin, Fan-Hsiu Chang, and Chih-Huang Lai

Citation: Applied Physics Letters **98**, 262507 (2011); doi: 10.1063/1.3603945
View online: http://dx.doi.org/10.1063/1.3603945
View Table of Contents: http://scitation.aip.org/content/aip/journal/apl/98/26?ver=pdfcov
Published by the AIP Publishing

Direct probing magnetization reversal of exchange-coupled-composite media by x-ray magnetic circular dichroism

Hao-Cheng Hou,[1] Dieter Suess,[2] Jung-Wei Liao,[1] Meng-Shian Lin,[1] Hong-Ji Lin,[3] Fan-Hsiu Chang,[3] and Chih-Huang Lai[1,a)]
[1]*Department of Materials Science and Engineering, National Tsing Hua University, 30013 Hsinchu, Taiwan*
[2]*Institute of Solid State Physics, Vienna University of Technology, 1040 Vienna, Austria*
[3]*National Synchrotron Radiation Research Center, 30076 Hsinchu, Taiwan*

(Received 19 March 2011; accepted 27 May 2011; published online 1 July 2011)

X-ray magnetic circular dichroism (XMCD) was used to directly probe the depth-dependent magnetization reversal of CoPtCr-SiO_2-based exchange-coupled-composite media with laminated soft layers. A thin Fe-marker layer in the soft layer was used as the indicator of local magnetization. Element-specific XMCD loops of Fe-marker layers confirmed the transition of the magnetization reversal from rigid magnets to exchange-spring magnets with increasing thickness of the soft layer. The micromagnetic simulations revealed the importance of the reduced exchange constant (A^{soft}) by laminating the soft layer for domain-wall assisting reversal. By comparing XMCD loops with simulations, we can deduce the effective A^{soft}. © *2011 American Institute of Physics*.
[doi:10.1063/1.3603945]

Exchange-coupled-composite (ECC) media, in which the columnar grains consist of a magnetically hard layer (HL) and a soft layer (SL), have been proposed to overcome the so-called magnetic recording "trilemma".[1,2] Various works have been demonstrated that the composite magnets enable us to improve writability without compromising thermal stability,[3] and to achieve superior recording performance.[4,5] To fully utilize the advantages of ECC media, complete understanding of the magnetization reversal mechanism is needed to optimize the layer structure. Several theoretical works have revealed that the transition from a rigid magnet (RM) to an exchange-spring magnet (ES) occurs as the SL thickness is increased.[6,7] To experimentally verify the reversal behavior of composite magnets, and to explore domain-wall (DW) assisting reversal of ES magnets, depth-dependent magnetization-probing techniques are required.

Several attempts have been made to probe magnetization in composite magnets or multilayers. Choi *et al.*[8] used the element-specific loops of x-ray resonant magnetic scattering to differentiate the incoherent reversal in each layer of the SmCo/Fe system. Kim *et al.* employed the x-ray magnetic circular dichroism (XMCD) with the standing wave modulation to study the depth-sensitive magnetization reorientation of Co/Pd interface,[9] and utilized the soft x-ray resonant magneto-optical Kerr effect to investigate the element- and interface-resolved magnetization reversal in exchange biased NiFe/FeMn/Co.[10] However, among these techniques, only the in-plane magnetization could be characterized. On the other hand, polarized neutron reflectometry (PNR) was used to reveal the domain wall formation in the perpendicular composite magnets,[11] however, modeling processes are required to interpret the PNR data and the magnetization configuration was typically obtained only at specific applied fields instead of sweeping fields. Consequently, a full reversal loop may not be provided by this technique.

In addition to understanding the magnetization reversal, to control the reversal behavior in ECC media, we may need to optimize the saturation magnetization (M_s), anisotropy constant (K_u), and exchange constant (A) of the HL and SL.[6] The M_s and the K_u can be tuned by changing the materials;[12] however, very few works have been focused on the influence and manipulation of the exchange constant of the SL (A^{soft}), because the range of A^{soft} among ferromagnetic materials is relatively limited.

In this letter, we report that we can directly probe the depth-dependent magnetization reversal in ECC media by using XMCD with a magnetization marker in the SL. We clearly demonstrate the transition of the reversal mode from RM to ES with respect to the SL thickness. In addition, results from micromagnetic simulations are consistent with the ES behavior observed in the XMCD loops. By comparing the results of simulations and XMCD loops, we further deduce the effective A^{soft} of the laminated SL, and show the importance of reduced A^{soft} on ES behavior.

All samples were prepared by DC magnetron sputtering. The magnetic layer, CoPtCr-SiO_2 (CPCS), was deposited with $Ar + O_2$ (0.5%) to ensure good grain isolation. The layer structure of the single-phase magnet, conventional perpendicular magnetic recording (called c-PMR hereafter) media, is substrate/Ta 3/Pt 7/Ru 15/CPCS 12/capped Pt 2 (unit: nm). The structure of the ECC media is substrate/Ta 3/Pt 7/Ru 15/CPCS 12/$[Pt\ 0.7/CPCS\ 1.1]_N$/capped Pt 2 ($N = 3$, 5, 7), in which CPCS and $[CPCS/Pt]_N$ are the HL and the SL, respectively. The laminated SL ($[Pt\ 0.7/CPCS\ 1.1]_N$) possesses the tunable inter-layer coupling and the controllable anisotropy by changing the Pt thickness.[13] To reveal the local reversal behavior, the magnetization marker layer (called Fe-marker layer hereafter) is inserted at different locations of SL by co-sputtering the CPCS (0.7 nm) and the Fe (0.4 nm). Since the Fe is strongly coupled to the CPCS layer, the out-of-plane XMCD loops of the Fe-marker layer, measured at Fe L_3 edge with the fluorescence yield mode, can reveal the local magnetization reversal of the SL. The

a)Author to whom correspondence should be addressed. Electronic mail: chlai@mx.nthu.edu.tw.

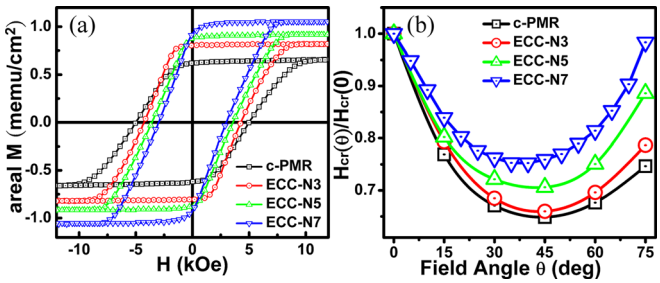

FIG. 1. (Color online) (a) Hysteresis loops and (b) normalized angular dependence of remanent coercivity $H_{cr}(\theta)/H_{cr}(0)$ on c-PMR and ECC with N = 3, 5, 7 ($H_{cr}(0)$ is measured at the out-of-plane direction.)

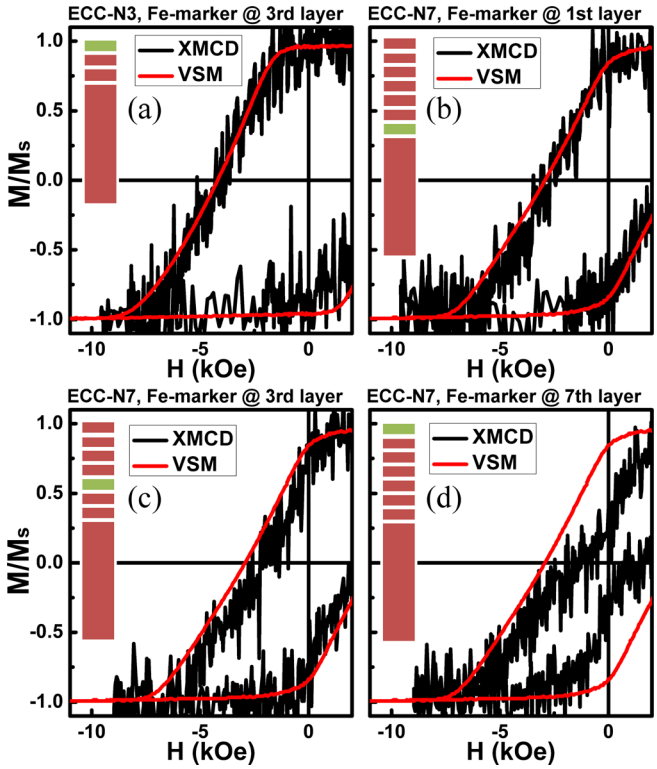

FIG. 2. (Color online) XMCD and VSM loops of (a) ECC-N3 with the Fe-marker in the 3rd layer, and of ECC-N7 with the Fe-marker in (b) 1st layer, (c) 3rd layer, and (d) 7th layer. Insets schematically show the CPCS layer with and without Fe-marker in different colors.

XMCD measurements of the Fe-marker layer were performed at the Dragon beam line 11A at the National Synchrotron Radiation Research Center. The hysteresis loops and remanent coercivity (H_{cr}) of ECC media were measured by using a vibration sample magnetometer (VSM).

The perpendicular hysteresis loops of ECC media with various SL thicknesses (N number) are presented in Fig. 1(a). The coercivity (H_c) and saturation field (H_s) in ECC media are reduced with increasing N. Figure 1(b) shows the angular dependence of normalized remanent coercivity $H_{cr}(\theta)/H_{cr}(0)$ for the samples with the N from N = 0 (c-PMR) to N = 7. For c-PMR, the curve can be characterized by a typical Stoner-Wohlfarth (SW)-like behavior that shows a symmetric curve with respect to 45°. The curve of ECC media with N = 3 (ECC-N3) is similar to that of the c-PMR, indicating that ECC-N3 exhibits a coherent switching, corresponding to the RM behavior. In contrast, ECC media with thicker SLs (N = 5 and N = 7) show angular dependences deviating from the SW model, which are often ascribed to the onset of the incoherent reversal.[2,5]

The element-specific XMCD provides a straightforward probing of the local Fe-marker, which enables us to investigate the depth-dependent magnetization reversal in the SL. The Fe-marker layer was inserted in the various designated locations in ECC-N3 and ECC-N7. We experimentally confirmed the ECC media behaved identically for samples with and without Fe-marker due to very limited amount of Fe. As schematically shown in the insets of Fig. 2, the green and red layers represent the CPCS layers with and without Fe-marker, respectively.

Figure 2(a) shows the hysteresis loops measured by VSM and XMCD for the ECC-N3 with the Fe-marker layer located at the 3rd layer of the SL (the top of the SL). Both the HL and the SL contribute to the signal of the VSM loop; the XMCD signal is only contributed from the Fe-marker layer so the XMCD loop is relatively noisy due to very limited amount of Fe. The XMCD loop reveals good coincidence with the VSM result, shown in Fig. 2(a), clearly demonstrating that even the top magnetization of SL is switched coherently with the whole ECC layers, corresponding to the RM behavior.

In Figs. 2(b)–2(d), XMCD and VSM loops are presented for the ECC-N7 with the Fe-marker layer located at various positions from the 1st to 7th layer. The VSM loops are all the same regardless of the position of Fe-marker layer. On the other hand, the XMCD loops taken from samples with the Fe-marker at different positions show depth-dependent switching behavior. The XMCD loop of the 1st layer (Fig. 2(b)) is nearly identical to the VSM one, indicating the strong coupling between the HL and the bottom of the SL. The XMCD loop of the 3rd layer (Fig. 2(c)) shows slightly reduced H_c compared to the VSM loop because the coupling to the HL is weakened. The distinctly different XMCD loop (Fig. 2(d)) is observed for the 7th layer (top of the SL); the sheared loop and the significantly reduced H_c confirm that the top of the SL is reversed at a lower field, providing the DW nucleation site to promote the DW assisting reversal. These results directly demonstrate the ES reversal along the depth-direction of the SL in the ECC-N7.

To further clarify the DW assisting reversal behavior, micromagnetic simulations were performed by using the simulation package FEMME.[7] Since the well isolated granular structures were observed in our ECC media, the simulations only considered the granular system with a weak inter-granular exchange coupling of $A_{\text{int}} = 1 \times 10^{-9}$ erg/cm. The transient states at various applied fields with A^{soft} of 0.35×10^{-6} erg/cm, shown in Fig. 3(a), depict the reversal of the ECC-N7. The following simulation parameters, corresponding to the film conditions, were considered: $M_s^{\text{hard}} = 550$ emu/cm^3, $M_s^{\text{soft}} = 302$ emu/cm^3, thickness $t^{\text{hard}} = 12$ nm, $t^{\text{soft}} = 12.6$ nm (N = 7), $K_u^{\text{hard}} = 4.4 \times 10^6$ erg/cm^3, $K_u^{\text{soft}} = -0.15 \times 10^6$ erg/cm^3, $A^{\text{hard}} = 1.0 \times 10^{-6}$ erg/cm, and $A^{\text{soft}} = 0.1$, 0.35, 0.5, and 1.0 ($\times 10^{-6}$ erg/cm). The anisotropy has a distribution of ± 10% and an angular distribution about the *c*-axis of 3°. Since the magnetic properties of ECC media are essentially the same regardless of the presence of the Fe-marker, it is

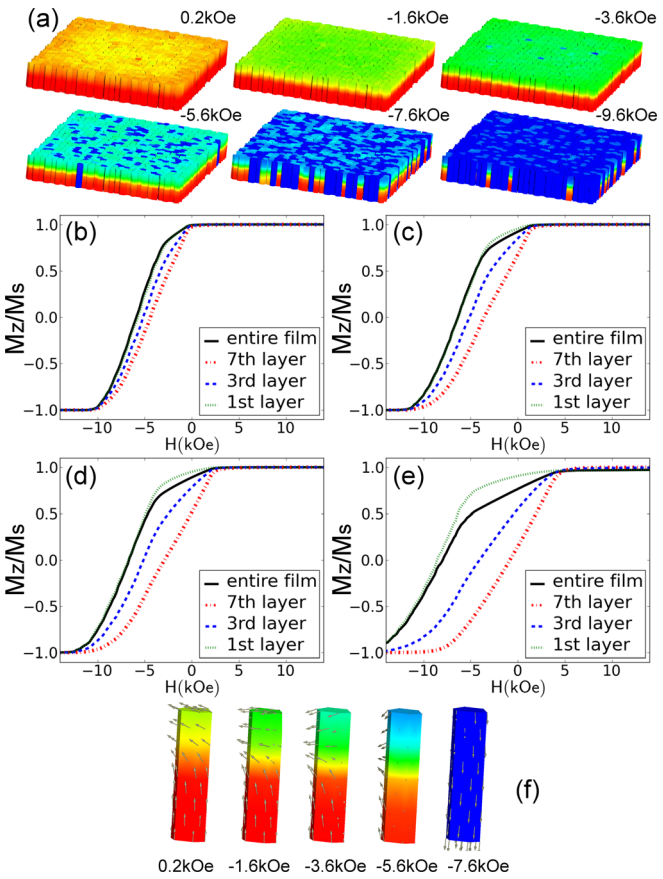

FIG. 3. (Color online) Simulation results of the ECC-N7 (a) transient states of the multi-grains at various fields in the case of $A^{soft} = 0.35 \times 10^{-6}$ erg/cm; the descending branches of hysteresis loop of the entire film (same as VSM curve in Fig. 2) and of the 1st, 3rd, and 7th layer in the SL of ECC-N7 with (b) $A^{soft} = 1 \times 10^{-6}$ erg/cm, (c) $A^{soft} = 0.5 \times 10^{-6}$ erg/cm, (d) $A^{soft} = 0.35 \times 10^{-6}$ erg/cm, and (e) $A^{soft} = 0.1 \times 10^{-6}$ erg/cm; (f) magnetization configuration at various fields of the ECC-N7 with $A^{soft} = 0.35 \times 10^{-6}$ erg/cm.

concluded that Fe played a negligible role. The effect of Fe-marker was not taken into account in the simulations.

It is worth mentioning that the laminated SL used in this study exhibits a tunable effective exchange constant because of the reduced interlayer coupling between successive CPCS layers through the Pt layer.[14] Figures 3(b)–3(e) show the ECC-N7 media with varied A^{soft} of 0.1, 0.35, 0.5, and 1 ($\times 10^{-6}$ erg/cm). The magnetization reversals of the three specific layers were captured in the simulations, corresponding to the 1st, 3rd, and 7th layer, similar to the experimental XMCD measurements. For the $A^{soft} = 1 \times 10^{-6}$ erg/cm, identical to the A^{hard}, all three layers show negative nucleation fields (H_n) and slightly reduced switching fields, which deviate from the XMCD results. According to Ref. 7, we estimated the required t^{soft} to form a full DW to be 21.2 nm for $A^{soft} = 1 \times 10^{-6}$ erg/cm; however, t^{soft} (12.6 nm) for N = 7 is smaller than the calculated value. This implies that the A^{soft} should be much less than 1×10^{-6} erg/cm. In Figs. 3(c)–3(e), simulations show that further reducing A^{soft} leads to more variations between the reversal curves of the SL taken from varied locations. If A^{soft} is reduced to 0.1×10^{-6} erg/cm (Fig. 3(e)), the exchange constant is so weak that only the bottom of the SL strongly couples to HL, revealing an extremely low H_s for the top (7th) layer. On the other hand, in Figs. 3(c) and 3(d), simulations show the positive H_n, the significantly reduced H_c and the comparable H_s between the entire film and the 7th layer, similar to the observed XMCD loops. From this, we deduce that the A^{soft} in the laminated SL ranges between 0.35 and 0.5 ($\times 10^{-6}$ erg/cm), which is lower than the typical single SL. With the deduced A^{soft} value of 0.35×10^{-6} erg/cm, Fig. 3(f) clearly shows that the DW nucleation, compression, and propagation take place in one of the ECC grains at varied fields.

In summary, we demonstrate direct evidence of the DW assisting reversal of ECC media by using XMCD measurements. Micromagnetic simulations confirm the onset of DW assisting reversal in the thinner SL is due to the reduced exchange constant by laminating the SL.

The authors would like to acknowledge China Steel Co. and ThinTech Materials Technology Co. for providing sputtering targets. This research was partially supported by the National Science Council of Republic of China under Grant No. NSC 98-2622-E-007-003, Ministry of Economic Affairs of Republic of China under Grant No. 99-EC-17-A-08-S1-006, and the FWF project ViCoM (F4112-N13) and WWTF MA09-029.

[1]R. H. Victora and X. Shen, IEEE Trans. Magn. **41**, 537 (2005).
[2]D. Suess, T. Schrefl, R. Dittrich, M. Kirschner, F. Dorfbauer, G. Hrkac, and J. Fidler, J. Magn. Magn. Mater. **290–291**, 551 (2005).
[3]D. Suess, T. Schrefl, S. Fahler, M. Kirschner, G. Hrkac, F. Dorfbauer, and J. Fidler, Appl. Phys. Lett. **87**, 012504 (2005).
[4]K. Tanahashi, H. Nakagawa, R. Araki, H. Kashiwase, and H. Nemoto, IEEE Trans. Magn. **45**, 799 (2009).
[5]J. P. Wang, W. K. Shen, and J. M. Bai, IEEE Trans. Magn. **41**, 3181 (2005).
[6]G. Asti, M. Ghidini, R. Pellicelli, C. Pernechele, M. Solzi, F. Albertini, F.Casoli, S. Fabbrici, and L. Pareti, Phys. Rev. B **73**, 094406 (2006).
[7]D. Suess, J. Magn. Magn. Mater. **308**, 183 (2007).
[8]Y. Choi, J. S. Jiang, J. E. Pearson, S. D. Bader, J. J. Kavich, J. W. Freel, and J. P. Liu, Appl. Phys. Lett. **91**, 072509, (2007).
[9]S. K. Kim and J. B. Kortright, Phys. Rev. Lett. **86**, 1347 (2001).
[10]S. K. Kim, K. S. Lee, J. B. Kortright, and S. C. Shin, Appl. Phys. Lett. **86**, 102502, (2005).
[11]S. M. Watson, T. Hauet, J. A. Borchers, S. Mangin, and E. E. Fullerton, Appl. Phys. Lett. **92**, 202507, (2008).
[12]A. J. Zambano, H. Oguchi, I. Takeuchi, Y. Choi, J. S. Jiang, J. P. Liu, S. E. Lofland, D. Josell, and L. A. Bendersky, Phys. Rev. B **75**, 144429 (2007).
[13]H. C. Hou, J. W. Liao, M. S. Lin, H. J. Lin, F. H. Chang, R. Z. Chen, C. H. Chiu, and C. H. Lai, J. Appl. Phys. **109**, 07C104 (2011).
[14]H. C. Hou, M. S. Lin, J. W. Liao, T. L. Wu, C. H. Lai, R. Z. Chen, J. L. Lee, H. J. Lin, F. H. Chang, and J. S. Yang, J. Appl. Phys. **105**, 07B729(2009).